Halteres for the Micromechanical Flying Insect *

W.C. Wu R.J. Wood R.S. Fearing

Department of EECS, University of California, Berkeley, CA 94720
{*wcwu, rjwood, ronf*}*@robotics.eecs.berkeley.edu*

Abstract

The mechanism which real flying insects use to detect body rotation has been simulated. The results show that an angular rate sensor can be made based on such a biological mechanism. Two types of biomimetic gyroscopes have been constructed using foils of stainless steel. The first device is connected directly to a compliant cantilever. The second device is placed on a mechanically amplifying fourbar structure. Both devices are driven by piezoelectric actuators and detect the Coriolis force using strain gages. The experimental results show successful measurements of angular velocities and these devices have the benefits of low power and high sensitivity.

1 Introduction

Micro aerial vehicles (MAVs) have drawn a great deal of attention in the past decade due to the quick advances in microtechnology. Commercial and military applications for micro-robotic devices have been identified including operations in hazardous environments, search-and-rescue within collapsed buildings, reconnaissance and surveillance, *etc.*. Although several groups have worked on MAVs based on fixed and rotary wings [6], flapping flight provides superior maneuverability that would be beneficial in obstacle avoidance and for navigation in small spaces [11].

Inspired by the exceptional flight capabilities achieved by real insects, the UC Berkeley Micromechanical Flying Insect (MFI) project uses biomimetic principles to develop a flapping wing MAV that will be capable of sustained autonomous flight. The overall structure of the MFI has been designed and some components have been built and tested [3],[10],[11]. As with real insects, angular rotation detection by the sensory system of the MFI is important for stabilizing flight. Although precise MEMS gyroscopes are commercially available, their designs (package size, power requirements, *etc.*) are in general not suitable for the MFI. On the other hand, piezoelectric vibrating structures have been developed and have proven to be able to detect Coriolis force with high accuracy [8]. Therefore, based on the gyroscopic sensing of real flies, a novel design using piezoelectric devices is being considered. This paper describes the simulations and fabrication of this type of biologically inspired angular rate sensor for use on the MFI.

*This work was funded by NSF KDI ECS 9873474, ONR MURI N00014-98-1-0671, and DARPA.

2 Haltere Morphology

Research on insect flight revealed that in order to maintain stable flight, insects use structures, called halteres, to detect body rotations via gyroscopic forces [5]. The halteres of a fly evolved from hindwings and are hidden in the space between thorax and abdomen so that air current has negligible effect on them (see figure 1). The halteres resemble small balls at the end of thin sticks. There are about 400 sensilla embedded in the flexible exoskeleton at the haltere base. These

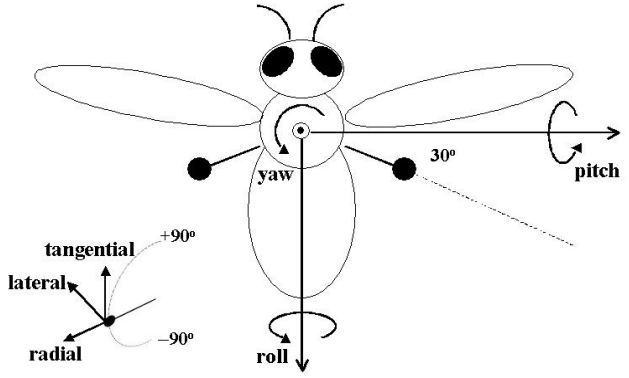

Figure 1: Schematic of enlarged halteres of a fly.

mechanoreceptors function as strain gages to detect the Coriolis force exerted on the halteres [4]. During flight the halteres beat up and down in vertical planes through an average angle of nearly 180^o anti-phase to the wings at the wingbeat frequency. When a fly's halteres are removed or immobilized, it quickly falls to the ground. In addition, the two halteres of a fly are non-

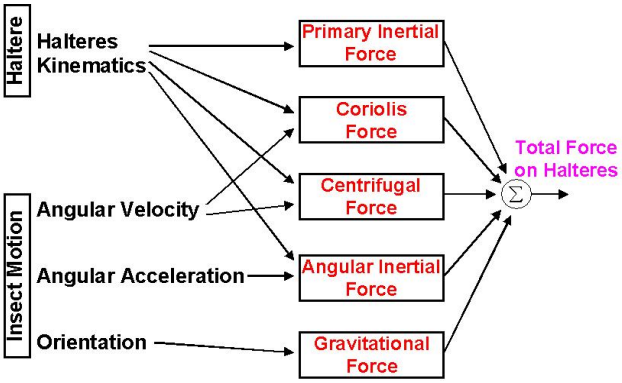

Figure 2: Haltere force modulation.

coplanar (each is tilted backward from the transverse plane by about 30^o) so that flies can detect rotations about all three turning axes.

As detailed in [7], a complex force, as a result of insect motion and haltere kinematics, acts on the halteres during flight (see figure 2). Assuming no translational motion of the insect, this force can be expressed in vector notation by the following:

$$\mathbf{F} = m\mathbf{g} - m\mathbf{a} - m\dot{\boldsymbol{\omega}} \times \mathbf{r} - m\boldsymbol{\omega} \times (\boldsymbol{\omega} \times \mathbf{r}) - 2m\boldsymbol{\omega} \times \mathbf{v} \quad (1)$$

where m is the mass of the haltere, $\mathbf{r}$, $\mathbf{v}$, and $\mathbf{a}$ are the position, velocity, and acceleration of the haltere relative to the insect body, $\boldsymbol{\omega}$ and $\dot{\boldsymbol{\omega}}$ are the angular velocity and angular acceleration of the insect, and $\mathbf{g}$ is the gravitational constant. Further, this force can be decomposed into radial, tangential, and lateral components as depicted by the exploded view of the haltere in figure 1. Insect's body rotations produce centrifugal ($-m\boldsymbol{\omega} \times (\boldsymbol{\omega} \times \mathbf{r})$) and Coriolis ($-2m\boldsymbol{\omega} \times \mathbf{v}$) forces on the halteres. The centrifugal force is generally smaller than the Coriolis force and mostly in the radial and tangential directions. Moreover, since the centrifugal force is proportional to the square of angular velocity of the insect, it provides no information on the sign of rotations. The Coriolis force, on the other hand, is proportional to the product of the angular velocity of the insect and the instantaneous haltere velocity. The Coriolis force has components in all three directions and contains information on the axis, sign, and magnitude of the insect's body rotation. The angular acceleration force ($-m\dot{\boldsymbol{\omega}} \times \mathbf{r}$) is proportional to the product of the angular acceleration of the insect and the instantaneous position of the haltere. The angular acceleration and the Coriolis force signals are separable because of the 90^o phase shift (they are orthogonal functions). The primary inertial force ($-m\mathbf{a}$) depends on the haltere acceleration relative to the insect body. This force is orders of magnitude larger than the Coriolis force and has only radial and tangential components. The gravitational force ($m\mathbf{g}$) is always constant and depending on the haltere position and the insect's body attitude in space, its distribution in the three directions varies. However, the effect of this gravitational force on the angular velocity sensing is negligible because it is a tonic lateral component which can be considered as DC offset on the Coriolis force and removed easily by the subsequent signal processing step.

3 Simulations

To detect angular rotations, the lateral forces on the halteres are measured because the large primary inertial force has no contribution in the lateral direction and hence it is possible to measure the Coriolis signal among all other interfering force signals appearing in this direction. Figure 3 shows the lateral components of the Coriolis force on both halteres for rotations about the roll, pitch, and yaw axes. Because of the dependence of the Coriolis force on the haltere velocity, these force signals are modulated in time with haltere beat frequency. For a roll rotation, the signal is modulated with the haltere beat frequency and the left and right signals are 180^o out-of-phase. For a pitch rotation, the signal is also modulated with the haltere beat frequency, but the left and right signals are in-phase. For a yaw rotation, the signal is modulated with double the haltere beat frequency and the left and right signals are 180^o out-of-phase.

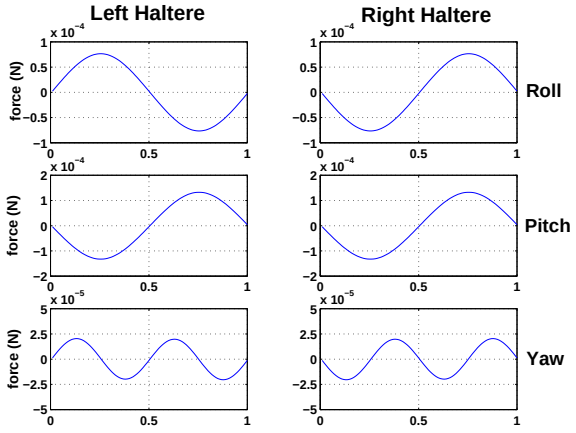

Figure 3: Coriolis lateral forces for rotations about roll, pitch, and yaw axes. Signals during one haltere cycle are shown.

Utilizing the characteristics (frequency, modulation, and phase) of these force signals on the left and right halteres, a demodulation scheme is proposed to distinguish roll, pitch, and yaw rotations. First, a

pitch rotation can be separated from roll and yaw rotations by adding the left and right signals. Because the left and right signals are in-phase for pitch while out-of-phase for roll and yaw, adding the left and right signals retains pitch component and eliminates roll and yaw components. Then, roll and yaw rotations can be separated by multiplying demodulating signals of different frequencies. A sinusoidal signal at the haltere frequency retrieves the roll signal while a sinusoidal signal of double the haltere frequency retrieves the yaw signal. Figure 4 illustrates the proposed demodulation scheme. Ideally, the magnitudes of the amplifiers, A_r, A_y, and A_p, would be proportional to $-1/2m$, where m is the mass of the haltere.

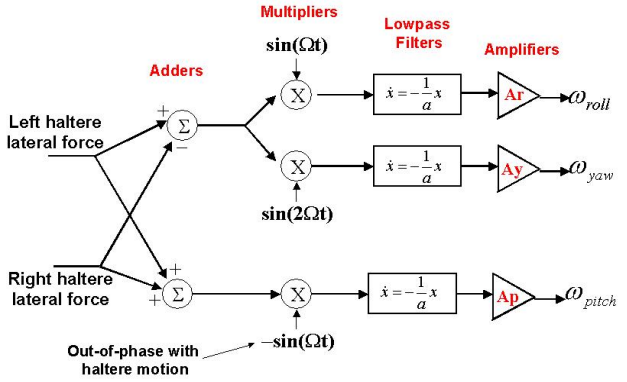

Figure 4: Demodulation scheme of haltere forces.

4 Haltere Design Issues

The results of the simulation show that a biomimetic mechanical haltere is feasible for the parameters of a robotic flying insect. The next step is to show with experimental results that it is feasible to use a mechanical haltere to measure angular velocity. To do this, the simulation parameters are used as the design parameters for the haltere. The key parameters for the design are the haltere length, mass, velocity, and stroke amplitude. Little attention is paid to the haltere orientation since it is assumed that it can be arbitrarily placed upon a robotic insect.

Unlike the force sensing methods used in [1],[2],[10], the haltere must have only one sensing degree of freedom. The design of the haltere must allow for high stiffness in the tangential direction and compliance in the lateral direction. Thus, the inertial forces will not be sensed, and the smaller Coriolis forces can be detected. The best case mechanically for this is a flat beam with the wide face in the plane of the haltere beating. The ratio of the stiffness in the two directions is given by the following:

$$\frac{k_t}{k_l} = \frac{\frac{EI_t}{3l^3}}{\frac{EI_l}{3l^3}} = \frac{I_t}{I_l} = \frac{\frac{bh^3}{12}}{\frac{hb^3}{12}} = \frac{b^2}{h^2} \tag{2}$$

where I_t and I_l are the tangential and lateral cross sectional moments of inertia, b is the width of the beam, and h is the thickness.

One of the major concerns with the design of the haltere is actuation. Since the Coriolis force is proportional to the haltere velocity, it is desired to have a high haltere beat frequency and a large stroke. Two methods of actuation will be discussed here. The simpler of the two places the haltere on a vibrating structure with a high Q compliant beam in between. The vibrating structure, in this case a piezoelectric actuator, drives the haltere into resonance, while its high Q gives large stroke amplitudes. This method has the benefits of not only being simple to construct, but also this structure has the ability to be driven parasitically from the body vibrations of the MFI. The second method places the haltere on the output link of a fourbar mechanism driven by a piezoelectric actuator, similar to the method used to drive the MFI wing as described in [3],[9],[11].

The first design to be discussed is the piezo-actuated vibrating structure. The mechanical haltere measures the Coriolis force using strain gages at its base which measure moments applied in the direction orthogonal to its beating plane. The first step in the haltere design is to determine from the simulation parameters what the minimum Coriolis force acting on the haltere will be. Using the simulation parameters of $400Hz$ beat frequency at an amplitude of $\alpha = 0.5rad$, and a length l of $5.5mm$, the peak velocity of the mass is found to be $2.27m/s$. Now, as a low-end estimate of a small angular velocity that a flying robotic insect will encounter, ω_{min} was set to $1rad/s$. Finally, the mass was set to $10mg$, so that the minimum Coriolis force acting on the mass is $22.7\mu N$.

The haltere can be thought of as a cantilever, with one end fixed at the point of rotation. Thus, the Coriolis force acting on the mass produces a strain in the beam defined by the following:

$$F_c = \frac{M}{l-x} = \frac{EI\epsilon}{z(l-x)} \tag{3}$$

where F_c is the Coriolis force, M is the generated moment, x is the distance from the base of the cantilever to the strain gage, E is the Young's modulus of the haltere material, I is the cross sectional moment of inertia, z is the distance from the neutral axis to the strain gage, and ϵ is the strain in the haltere. From

equation 3, it is clear that the maximum moment, and thus the maximum sensitivity will occur by placing the gage as close to the point of rotation as possible. The haltere is constructed in such a way that there is a high Q compliant section to allow for rotation, and then the beam is twisted to allow compliance in the desired direction. Thus, the minimum dimension x was constrained to be $2mm$. The modulus E is given to be 193 GPa since the material used was stainless steel. The cross sectional moment of inertia is defined to be $I = bh^3/12$, thus the final parameters to be determined for the haltere were b and h. Using a thickness of $50\mu m$ and a width of $0.5mm$, along with the minimum Coriolis force gives the minimum strain $\epsilon_{min} = 2\times10^{-6}$ which is above the noise floor for typical strain gage signal conditioners. Also, from equation 2, the ratio of tangential to lateral stiffness is 100. For actuation, the haltere was connected directly to the free end of a cantilevered PZT unimorph. This was done in such a way that the Q of the haltere was sufficiently high to allow for greater motion than that of the PZT alone.

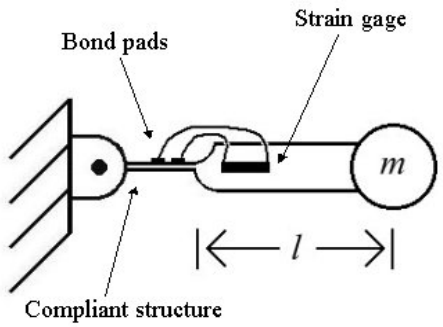

Figure 5: Haltere description and design parameters.

The last design issue was how to orient the strain gages and deal with their wires. Since the gages are extremely sensitive to thermal drifts, a full *Wheatstone Bridge* is the most desirable configuration for the sensors. However, because of the limited surface area of the haltere, only a half bridge was possible. This was done by placing one gage on either side so that one would always be in compression while the other was in tension. The sensors used were $1mm$ long $\times$ $100\mu m$ wide semiconductor strain gages made by Entran, Inc. The main concern with the gage placement is successfully using the delicate gold leads to bring the signal off the haltere while not damaging them or adding additional parallel stiffness to the structure. This was done by placing bond pads on the compliant end of the haltere as shown in figure 5. The lead wires were fixed to these pads and more sturdy wire was coiled and connected to the pads. Figure 6 shows the completed haltere.

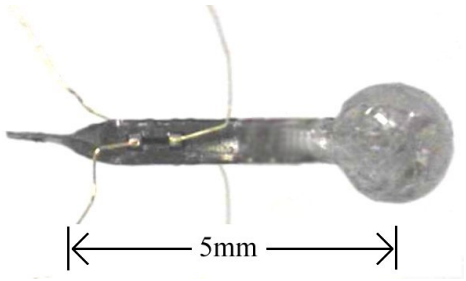

Figure 6: Completed haltere with half bridge strain sensor.

The design of the second haltere is similar to the design of the MFI thorax structure as is described in [3]. Instead of driving the haltere from a vibrating structure, it is placed on the output link of a mechanically amplifying fourbar structure. The fourbar takes the small linear displacement of the actuator and transforms this into large angles at the output [3],[11]. This technique gives better control over the motion of the haltere, allowing for large stroke amplitudes at high resonant frequencies. Since the Coriolis force acting on the haltere mass is proportional to the haltere velocity, this method of actuation should give greater sensitivity for detection of body angular velocity.

Assuming similar kinematic and dynamic constraints as the MFI thorax, 120^o stroke amplitude at $150Hz$, and resolution constraints for sensing the forces, there are again four parameters to determine. Three geometric parameters and the mass of the haltere are constrained by four defining equations. First, it is desired that the stiffness in the lateral direction of the haltere is significantly higher than the drive frequency so that the lateral resonant mode is not excited during actuation. Setting the lateral resonant frequency at $500Hz$ gives the following:

$$2\pi \cdot 500 = \sqrt{\frac{k_l}{m}} = \sqrt{\frac{Ebh^3}{4l^3m}} \tag{4}$$

where k_l is the lateral stiffness, m is the mass of the haltere (again assumed to be greater than the cantilever mass), E is the modulus of the material used, and b, h, and l are the width, thickness, and length of the cantilever, respectively. Next, the minimum Coriolis force is given as a function of the minimum detectable strain.

$$F_{c\min} = \frac{Ebh^3}{6l}\epsilon_{\min} \tag{5}$$

For the given kinematic parameters and the desired drive frequency, the haltere velocity is $200\pi \cdot l$. Now

from equation 1, the minimum Coriolis force can be related to the minimum detectable angular velocity (again assumed to be $1rad/s$) by the following:

$$F_{c\text{min}} = 2m\omega_{\text{min}} \times \text{v} = 400\pi \cdot m \cdot l \qquad (6)$$

Equating equations 5 and 6 gives the following:

$$Ebh^3\epsilon_{\text{min}} = 2400\pi \cdot m \cdot l^2 \qquad (7)$$

where the minimum detectable strain is a known parameter. The last constraint is from the dynamics of the MFI thorax and is based upon the desired MFI wing inertia. Equating the haltere inertia with the wing inertia gives the following:

$$J = m \cdot l^2 \qquad (8)$$

The inertia of the haltere, $J = 40mg\text{-}mm^2$, is only twice the MFI wing inertia [11]. Choosing $b = 1mm$ because of geometric constraints of the fourbar gives three unknown parameters to be solved from equations 5, 7, and 8. Choosing $m = 4mg$, $l = 5mm$, and $h = 50\mu m$ gives a close fit to the three constraints, while still considering construction difficulties.

5 Experimental Setting

5.1 Test Setup

To test the first haltere, it was setup on a servo motor, oriented such that at rest the haltere was along the ω-axis. This experiment would be equivalent to sensing the pitch angular velocity. The servo motor had an angular velocity range of approximately $0.1 - 10rad/s$. Ideally, the motor would be allowed to freely rotate to sense a pure angular velocity. However, for wiring concerns, the range of motion was restricted. One concern in the actuation of the haltere was to orient the haltere on the actuator such that when there was an applied angular velocity, the inertial force of the haltere would not interfere with the sensed signal. However, assuming perfect alignment, the inertial force sensed by the haltere at $\omega = 1rad/s$ is $m\omega^2 sin(\alpha/2) = 2.59\mu N$, roughly an order of magnitude lower than the Coriolis force. Much care was taken to ensure that the haltere was aligned directly along the ω-axis. The fourbar driven haltere was tested in a similar manner to the first haltere. However, to obtain a smother angular velocity, the structure was placed on a harmonic oscillator. The position of the structure on the oscillator was determined by using high-speed video footage and some simple image processing. After construction, the haltere resonant frequency was found to be $70Hz$, at a stroke amplitude of 90^o. This haltere structure can be seen in figure 7.

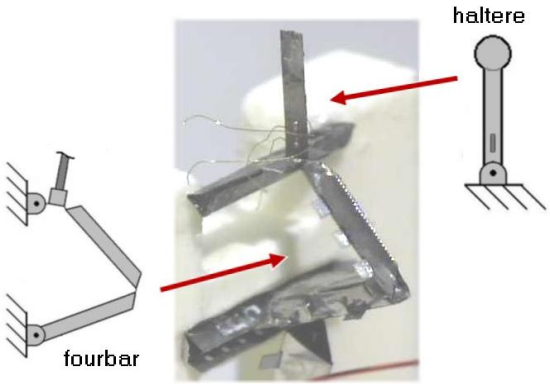

Figure 7: Fourbar actuated haltere at rest.

5.2 Results

The experimental results for the first haltere setup showed that the haltere detects both the Coriolis force and the inertial force of the mass. Figure 8 shows the measured angular velocity and the angular velocity of the motor. The measured signal was demodulated as described in Section 3. First, the signal was multiplied with a unity magnitude *sine* wave of precisely the haltere frequency and phase. Note that the haltere phase was not measured because position sensors for the haltere are difficult to implement on such a small scale. Instead, the actuator phase was measured, and since the haltere is at resonance, it is assumed that its phase lags 90^o behind that of the actuator. Then, this demodulated signal was filtered with a 3^{rd} order *Butterworth* lowpass filter with a cutoff frequency of $4Hz$ to eliminate remaining high frequency noise.

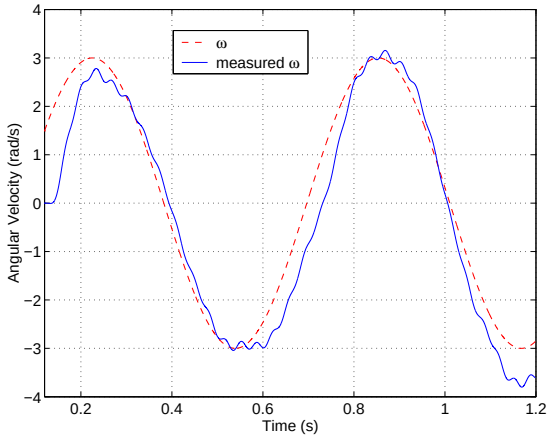

Figure 8: Pitch detection by the first haltere.

The results for the second structure are seen in figure 9. One key difference between the two is that with the fourbar driven structure, the position of the haltere

can be sensed using actuator-mounted strain sensors as described in [10]. After testing, this position was normalized to yield a unity magnitude *sine* wave which represented the haltere phase. This was then used to demodulate the signal using the same demodulation scheme as the first structure.

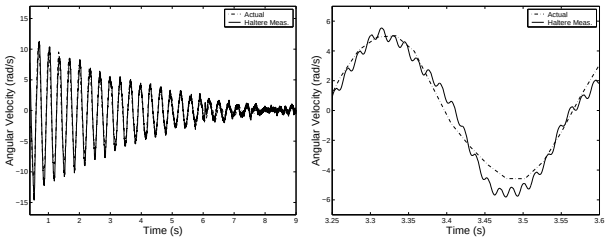

Figure 9: (a) Result for the fourbar actuated haltere; (b) Zoomed in to show accuracy.

6 Conclusions and Future Work

There are several advantages for the MFI in using halteres instead of MEMS gyroscopes as angular rate sensors. First, the haltere needs very little power since it does not use active actuation. It can be driven parasitically from the body vibrations when it is placed on the MFI body. Second, the haltere has a large dynamical range. It can detect angular velocities from as low as tens of degrees per second to as high as hundreds of thousands of degrees per second, which is often encountered during sharp turns of flying insects. Finally, when the wings of the MFI are flapping, the wing inertia will cause the MFI body to oscillate about the axis perpendicular to the stroke plane. The haltere can reduce the error caused by these oscillations by phase-locking to the wing. Table 1 shows a comparison of the halteres to a MEMS gyroscope made by Irvine Sensors Corp. In future revisions, the wiring of the haltere will be passed through slip rings such that the entire structure is free to rotate during testing. In addition, two halteres will be used together and oriented differently along the ω-axis to sense each of the three angular velocities and further test the demodulation techniques.

	Haltere I[1,2]	Haltere II[1,2]	MEMS Gyro[3]
Mass (mg)	12	30	1
Res. ($^o/s$)	50	50	6
Max Rate ($^o/s$)	$\pm 100,000$	$\pm 300,000$	± 60
B.W. (Hz)	5	15	10
Power (mW)	1	1	45

1 Assuming parasitic drive.
2 Assuming 1% duty cycle strain gage sampling.
3 Using thinned Si micromachined device.

Table 1: Comparison of different angular rate sensors.

Acknowledgments

The authors thank M. Dickinson for insight into the haltere physiology and dynamics, S. Avadhanula and L. Schenato for helpful discussions on the haltere design and simulations.

References

[1] K. Abe, T. Miwa, and M. Uchiyama. Development of a 3-axis planar force/torque sensor for very small force/torque measurement. *Trans Jpn Soc Mech Eng*, 42(2):376–382, 1999.

[2] A. Bicchi, A. Caiti, and D. Prattichizzo. Optimal design of a multi-axis force/torque sensor. In *Proc of the IEEE International Conference on Decision and Control*, pages 2981–2986, Phoenix, AZ, Dec 1999.

[3] R.S. Fearing, K.H. Chiang, M.H. Dickinson, D.L. Pick, M. Sitti, and J. Yan. Wing transmission for a micromechanical flying insect. In *Proc of the IEEE International Conference on Robotics and Automation*, pages 1509–1516, San Francisco, CA, April 2000.

[4] G. Fraenkel and J.W.S. Pringle. Halteres of flies as gyroscopic organs of equilibrium. *Nature*, 141:919–921, 1938.

[5] R. Hengstenberg. Mechanosensory control of compensatory head roll during flight in the blowfly Calliphora erythrocephala Meig. *Journal of Comparative Physiology A*, 163:151–165, 1988.

[6] B. Motazed, D. Vos, and M. Drela. Aerodymatics and flight control design for hovering MAVs. In *Proc of Amer Control Conference*, Philadelphia, PA, June 1998.

[7] G. Nalbach. The halteres of the blowfly Calliphora: I. kinematics and dynamics. *Journal of Comparative Physiology A*, 173:293–300, 1993.

[8] H. Sato, T. Fukuda, F. Arai, H. Iwata, and K. Itoigawa. Analysis of parallel beam gyroscope. In *Proc of the IEEE International Conference on Robotics and Automation*, pages 1632–1637, Detroit, MI, May 1999.

[9] M. Sitti, D. Campolo, J. Yan, R.S. Fearing, T. Su, and D. Taylor. Development of PZT and PZN-PT based unimorph actuators for micromechanical flapping structures. In *Proc of the IEEE International Conference on Robotics and Automation*, pages 3839–3846, Seoul, South Korea, May 2001.

[10] R.J. Wood and R.S. Fearing. Flight force measurement for a micromechanical flying insect. In *Intelligent Robots and Systems*, Maui, HI, Oct 29-Nov 3 2001.

[11] J. Yan, R.J. Wood, S. Avadhanula, R.S. Fearing, and M. Sitti. Towards flapping wing control for a micromechanical flying insect. In *Proc of the IEEE International Conference on Robotics and Automation*, pages 3901–3908, Seoul, South Korea, May 2001.